COBISS: 1.01, DOI:10.3986/ac.v51i1.10454

CAVES, SINKHOLES, AND FRACTURES IN THE EOGENETIC KARST OF FLORIDA, A GIS-BASED SPATIAL ANALYSIS

JAMA, VRTAČE IN RAZPOKE V EOGENEM KRASU FLORIDE, PROSTORSKA ANALIZA Z ORODJI GIS

Can DENIZMAN[1*]

Abstract UDC 551.435.8:659.2:004:91(735.9)
Can Denizman: Caves, sinkholes, and fractures in the eogenetic karst of Florida, a GIS-based spatial analysis
The correlation between surface and subsurface karst development was explored by comparing the directionality and spatial distribution of karstic depressions around twenty-two select caves in the eogenetic karst of Florida. Orientations of cave passages and major axes of depressions around cave centrelines imply varying degrees of correlation between them. Spatial distribution of karstic depressions was studied by standard deviational ellipses of sinkhole centroids and nearest neighbour orientations around caves using spatial statistics tools of ArcGIS. An overall analysis of the data shows close connections between some caves and the surrounding sinkholes in terms of their orientation and spatial distribution, suggesting the importance of fracture systems in the development of karst.
Keywords: karst geomorphology, caves, sinkholes, GIS, spatial analysis, Florida.

Izvleček UDK 551.435.8:659.2:004:91(735.9)
Can Denizman: Jame, vrtače in razpoke na eogenem krasu na Floridi, prostorska analiza z orodji GIS
Z analizo smeri in prostorske porazdelitve vrtač v okolici 22 izbranih jam na eogenem krasu na Floridi smo raziskovali povezavo med površinskim in podzemnim razvojem krasa. Primerjava smeri jamskih rovov in glavnih osi vrtač v okolici jam kaže na različno stopnjo povezave med njimi. Prostorsko porazdelitev vrtač smo raziskovali z orodji prostorske statistike v okolju ArcGIS, pri tem smo uporabili elipse standardnih odklonov centroidov vrtač in smeri osi vrtač, najbližjih sosedov izbranih jamskih rovov. Celotna analiza podatkov je pokazala tesno povezanost med nekaterimi jamami in okoliškimi vrtačami z vidika njihove orientacije in lege, kar kaže na pomen razpoklinskih sistemov za razvoj krasa.
Ključne besede: kraška geomorfologija, jame, vrtače, GIS, prostorska analiza, Florida.

[1] Department of Physics, Astronomy, Geosciences, and Engineering Technologies, Valdosta State University, 1500 Patterson Street, GA-31698, Valdosta, Georgia, USA, e-mail: cdenizma@valdosta.edu
* Corressponding author

Received/Prejeto: 18.10.2021

1. INTRODUCTION

Karst in Florida developed within the thick and porous Eocene and Oligocene limestones of a stable carbonate platform. The lack of significant tectonic activity gave rise to a well-developed karst plain with very little relief, which was later covered by siliciclastic material (White, 1970; Scott, 1997). The development of a surficial drainage network on the impermeable siliciclastic cover not only increased hydraulic gradient by river downcutting, contributing to karst groundwater circulation and conduit development but also eroded the impermeable cover material along the Suwannee River (Denizman & Randazzo, 2000). Allogenic recharge to the exposed carbonate platform and the subsequent hydrogeologic connection between surface and subsurface karst, a common characteristic of epigenetic karst areas, is readily observed in Florida by the sinkhole-cave-spring continuum (Kincaid, 1998) as well as groundwater flow within a maze of passages and rock matrix (Florea, 2006). Hypogenic karst development due to various processes such as groundwater – seawater mixing during low sea-level stands was proposed to explain deeper cave horizons (Moore et al., 2010; Gulley et al., 2013). With no significant burial diagenesis, carbonate rocks of Florida still retain their intergranular (matrix) porosity and form a perfect example of eogenetic karst as defined by Vacher and Mylroie (2012). Groundwater storage and flow take place within the dual porosity of the eogenetic karst aquifers which may not show a strong connection with the regional structural features and surficial karst development. Nevertheless, fracture patterns seem to be playing an important role in cave development with crude branchwork patterns within the undeformed Tertiary carbonates of the eogenetic Florida karst (Florea &Vacher, 2006; Palmer, 2009; Upchurch et al., 2019). The importance of structural features such as faults, fractures, and bedding planes on karst development, as well as the connection between subsurface and surficial karst processes, have been reported especially in telogenetic karst areas with little matrix porosity due to burial and diagenesis (e.g., Ford,

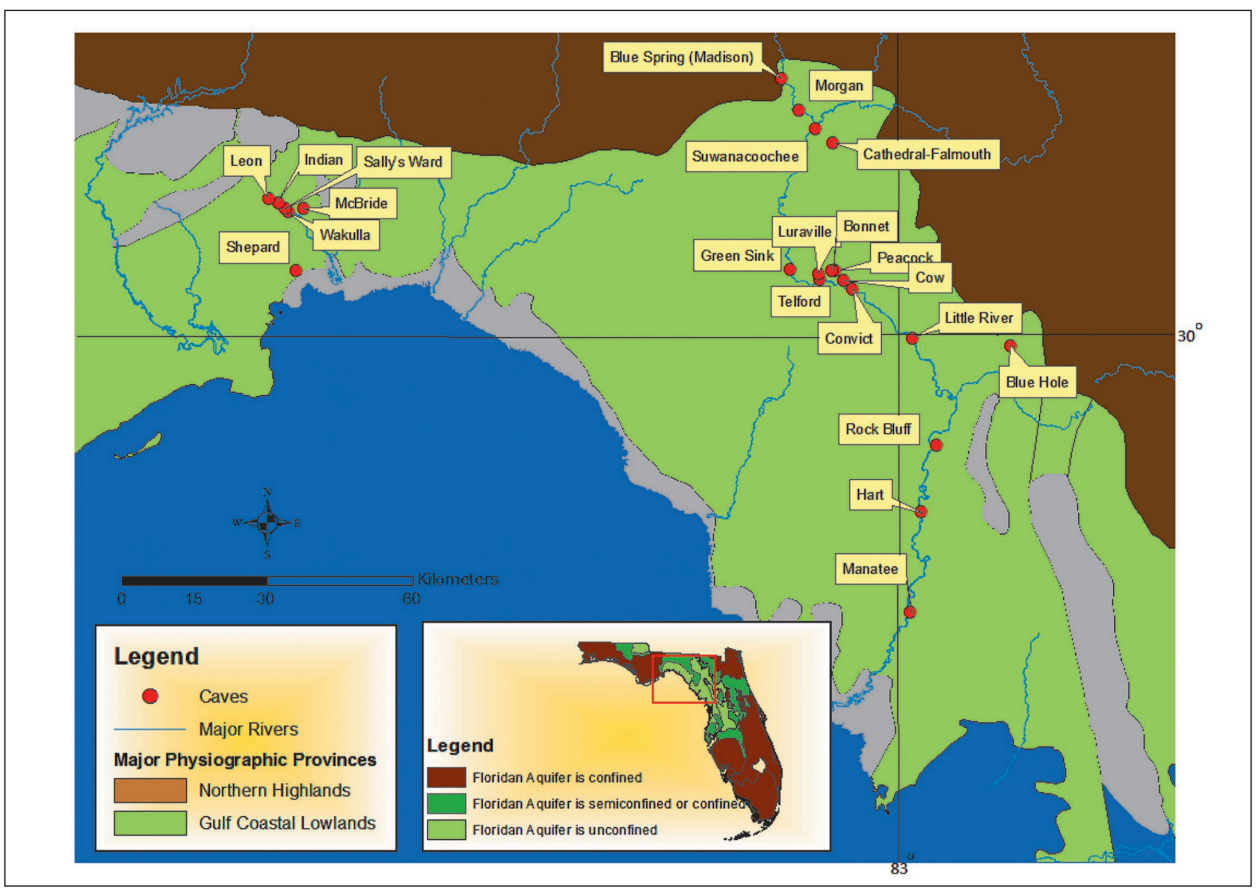

Figure 1: Major physiographic provinces and cave locations. Gray areas show minor physiographic provinces such as Coastal Swamps, Brooksville Ridge and Bell Ridge.

1964; La Velle, 1967; Palmer & Palmer, 1975; Kemmerly, 1982; Barlow & Ogden, 1982; Shofner et al., 2001; Favre & Pahernic, 2007). This study aims to explore the relationship between the caves and karstic depressions in the eogenetic karst of Florida by analyzing the spatial distribution and directional patterns of selected caves and surrounding karstic depressions. Analysis of large sets of spatial data was made possible by utilizing GIS as in many other studies on the spatial analysis and morphometric features of karst features (e.g., Denizman, 2003; Angel et al., 2004; Lyew-Ayee et al., 2009; Komac & Urbanc, 2012; Öztürk et al., 2018).

2. PHYSIOGRAPHY AND STRUCTURAL GEOLOGY OF THE STUDY AREA

Karst in Florida has developed within the undeformed Eocene and Oligocene carbonates of high primary porosity and rather uniform stratigraphy which can only be differentiated by biostratigraphy (Randazzo, 1997).

The Northern Highlands and Gulf Coastal Lowlands constitute the major physiographic provinces in the area (Figure 1). As one of the most distinct physiographic features in Florida, the Northern Highlands occupies most of the north and east of the study area. From the hydrogeologic standpoint, the Northern Highlands contains a thick confining unit of siliciclastic sediments and generates confining conditions for the Floridan aquifer. The confining unit originally covered the entire study area and has been eroded by headward erosion through surface drainage as well as by karstic dissolution within the underlying carbonate units (Scott, 1997).

The Gulf Coastal Lowlands consists of both erosional and depositional features. Broad plains of a series of Pleistocene surfaces and shorelines are pitted with karstic depressions within the limestone at or near land surface. The Floridan aquifer is unconfined. It represents a typical mature karst terrane with a thin mantle of permeable marine terrace deposits. Because of the low topographic relief and rapid infiltration of rainfall by diffuse recharge to the karst aquifer, surficial runoff is limited to major rivers. Well-developed epikarst provides the initial stages of subsurface karst development (Upchurch et al., 2019).

The Cody escarpment separates the Northern Highlands from the Gulf Coastal Plain and plays a major role in karst development along the retreating marginal zone between the two physiographic provinces. Allogenic recharge from the noncarbonate cover sediments of the Northern Highlands accounts for extensive dissolution, resulting in disappearing streams and collapse features above major solutional conduits (Figure 2). Numerous cave diving expeditions and tracing experiments have revealed an intricate network of karst development represented by caves, disappearing streams, sinkholes, and springs (Figure 3; Kincaid, 1998).

Figure 2: A disappearing stream in Leon Sinks State Park, Florida.

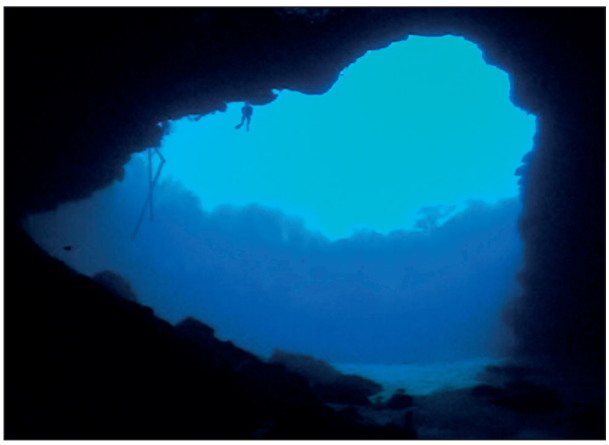

Figure 3: Wakulla Springs cave entrance.

Structural control on the drainage patterns and sinkhole alignments have been reported in various studies on the geomorphology of the Florida platform. Vernon (1951) proposes stresses that form the folds of the Ocala Uplift (Platform) to be the cause of the regional fracturing and mentions NW and NE system of fractures paralleling stream patterns and sinkhole alignments. These fractures are thought to have been formed by the tensional stresses over the anticlinal flexure.

Upchurch et al. (2019) suggest that the fractures due to tidal and tectonic stresses develop as soon as the carbonates are cemented and thus represent brittle characteristics. They propose tidal stresses as possible causes of fracture development rather than tectonic movement.

3. DATA

Spatial correlation between subsurface and surface karst development was explored by comparing the alignment of cave passages with major axes of karstic depressions and spatial distribution of depression centroids around caves.

3.1 CAVE DATABASE

Data on subsurface karst development comprise a Geographic Information System (GIS) database of twenty-two phreatic caves located within the Gulf Coastal Lowlands physiographic province where the Floridan aquifer is unconfined (Figure 1). GIS layers of caves, created by digitizing the centerlines of cave passages in ArcGIS contain information on average dimensions and depths of cave segments. All the caves are phreatic and most are located along the Suwannee and Wakulla rivers.

3.2 KARSTIC DEPRESSIONS DATABASE

The surficial karst development is analyzed by the spatial distribution of karstic depressions. Data on karstic depressions were compiled from four different sources:

1. Topographic maps: Most of the depressions used in this study were digitized as polyline layers from 1/24,000 topographic maps. Each depression is represented by its GIS-determined centroid point.
2. Florida sinkhole database: Maintained by the Florida Geological Survey, this database is comprised of reported subsidence incidents statewide.
3. Digital soil maps: SSURGO GIS soils data set includes some spatial point data that are potentially useful, especially since they are based on the direct field observations of the soil mappers. The soils survey reports use the terms "depression" and "sinkhole" interchangeably to an extent since they are both defined on the basis of closed depressions.
4 2-ft topographic contours derived from the LIDAR data by the Florida Division of Emergency Management. This GIS layer was available only for the northwest corner of the study area around the following caves: Wakulla, Leon, Sally's Ward, Indian, Shepherd, and McBride.

In the field, a total of 244 fracture orientations along the Suwannee River were measured and displayed in rose diagrams.

4. SPATIAL ANALYSIS OF THE DATA

Spatial analyses of the data include calculating length and orientation of cave passages and hundreds of depression major axes around the caves, determining points of depression centroids, and their spatial distribution properties on a GIS platform.

To explore the directional correlation between surface and subsurface karst development, depressions within 2 and 3 km of cave centerlines were used. Major axis azimuths of depressions with major axis-minor axis ratio >= 1.5, measured by ArcGIS using a

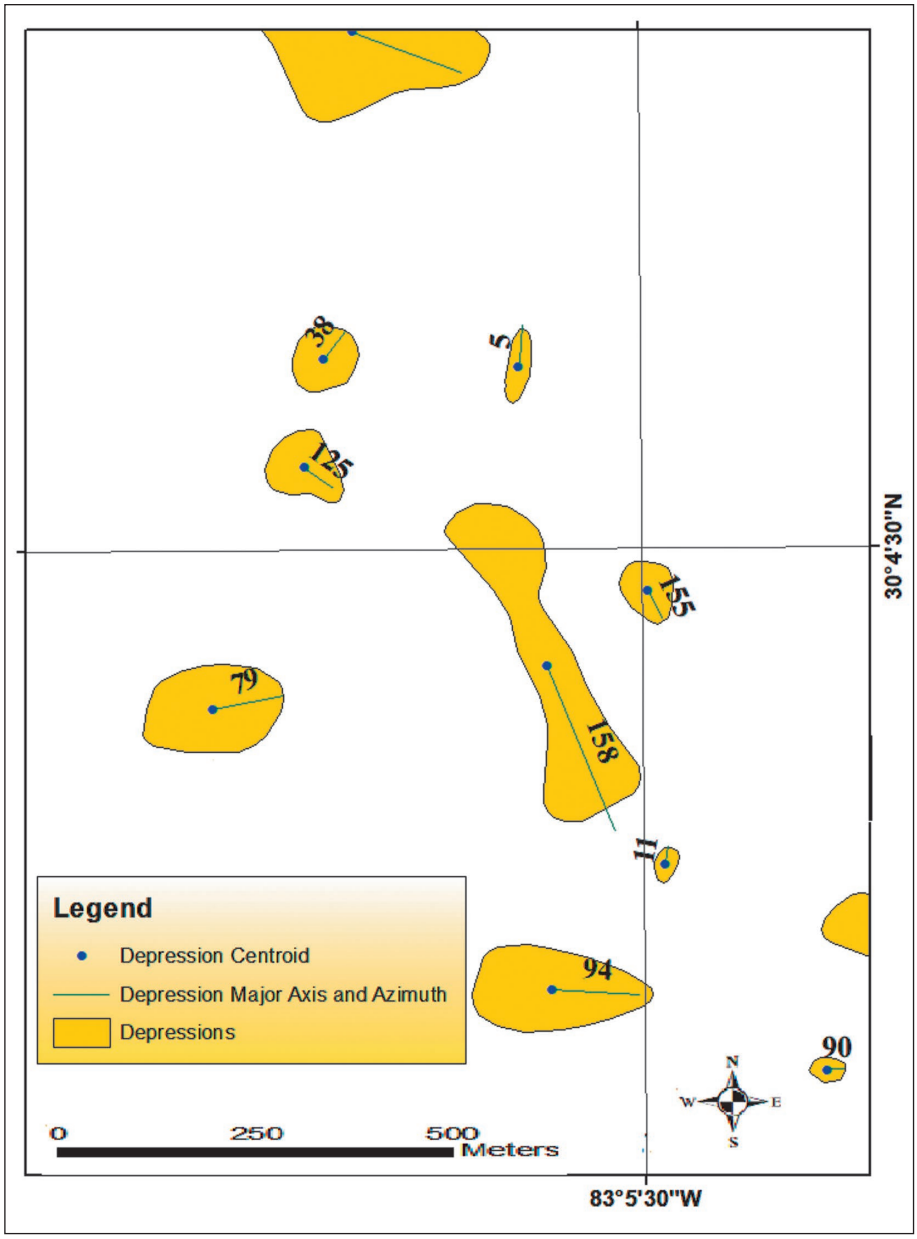

Figure 4: Examples of depression major half axes and centroids. Numbers denote major half axis azimuth angles.

fitted ellipse to the depression polygon, were calculated and compared with the azimuths of cave passages (Figure 2).

Using the spatial statistics tools of ArcGIS 10.4, spatial orientation of depression centroids located within distances of 1, 2, and 3 kilometers from the cave centerline were analyzed. Spatial orientation, or trend of depression point distribution was determined by calculating the standard distance separately in X and Y directions. These two measures make up the axes of an ellipse that describe the distribution of features. The ellipse, referred to as standard deviational ellipse (SDE), represents the standard deviation of the features from the mean center separately for the X and Y coordinates. It is expressed as (Equation 1):

$$SD_x = \frac{\sqrt{\sum(x_i - \bar{x})^2}}{n} \qquad SD_y = \frac{\sqrt{\sum(y_i - \bar{y})^2}}{n} \qquad (1)$$

where SD_x and SD_y are standard distances for the x and y axes, x_i, y_i, , and represent x and y coordinates of a feature and the mean x, y coordinates, and n is the number of features (Mitchel, 2005).

Spatial distribution of depression centroids was also analyzed by calculating azimuth values between nearest neighbors.

5. RESULTS AND DISCUSSIONS

Table 1 shows an overall summary of the cave morphology as related by Palmer (1991, 2009) to recharge type and the dominant porosity. The nearest neighbor index patterns for depressions within 3 km of each cave, the degree of alignment between each cave, and the spatial deviation ellipses (SDE) for depressions within 1, 2, and 3 km of the cave centerline are also included in this table. All the porosity types cited in Palmer's diagram –fracture, bedding planes, and the intergranular porosity- are observed in caves examined in this study.

Figure 5 allows a comparison of alignments among cave centerlines, nearest neighbor azimuths, SDE for depressions, and depression major axes within 2 and 3 km of the cave centerlines. In general, moderate to good correlation of alignments are observed between the rose diagrams of cave passages and the nearest neighbor azimuths within 2 km of the following caves: Bonnet, Cow- and the SDEs for the following caves: Bonnet, Cow, Leon, Litle River, Luraville, McBride, Morgan, Peacock, Shepard, Suwanacoochee, and Wakulla.

Table 1: Cave patterns and spatial distribution of sinkhole centroids (# :Number, NN: Nearest Neighbor, SDE: Standard Deviational Ellipse). Number of sinkholes within 2 and 3 km of caves are separated by semi-colon.

Cave	Pattern	Dominant Control	# of Sinkholes with L/W>=1.5 in 2 and 3 km	NN Pattern in 3 km	SDE Alignment
Blue Hole	Angular	Fracture	16; 115	Random	Poor
Bonnet	Anastomoses + angular	Bedding plane partings + fractures	51; 162	Random	Poor
Cathedral-Falmouth	Angular	Fracture	313; 927	Clustered	Perfect
Convict	Angular + rudimentary branchwork	Fracture + intergranular	43; 152	Random	Poor
Cow	Angular + rudimentary branchwork	Fracture + intergranular	51; 116	Random	Moderate
Green	Curvilinear passages	Bedding plane partings	80; 245	Random	Poor
Hart	Anastomoses	Bedding plane partings	50; 104	Clustered	Perfect
Indian	Angular + Curvilinear passages	Fracture + bedding plane partings	137; 430	Clustered	Poor
Leon	Angular + rudimentary branchwork	Fracture + intergranular	460; 745	Clustered	Perfect
Little River	Angular + rudimentary branchwork	Fracture + intergranular	67; 195	Clustered	Good
Luraville	Angular	Fracture	172; 322	Clustered	Good
Madison Blue	Angular + rudimentary branchwork	Fracture + intergranular	16; 39	Clustered	Good
Manatee	Angular	Fracture	61; 140	Clustered	Perfect
McBride	Angular	Fracture	192; 361	Clustered	Good
Morgan	Angular	Fracture	43; 110	Clustered	Good
Peacock	Anastomoses + angular	Bedding plane partings + fractures	64; 186	Clustered	Poor
Rock Bluff	Angular + rudimentary branchwork	Fracture + intergranular	35; 128	Clustered	Moderate
Sally's Ward	Angular	Fracture	162;392	Clustered	Good
Shepard	Angular	Fracture	211; 462	Clustered	Moderate
Suwanacoochee	Angular + rudimentary branchwork	Fracture + intergranular	99; 185	Clustered	Perfect
Telford	Angular + rudimentary branchwork	Fracture + intergranular	79; 249	Random	Good
Wakulla	Angular + Curvilinear passages	Fracture + bedding plane partings	317; 607	Clustered	Perfect

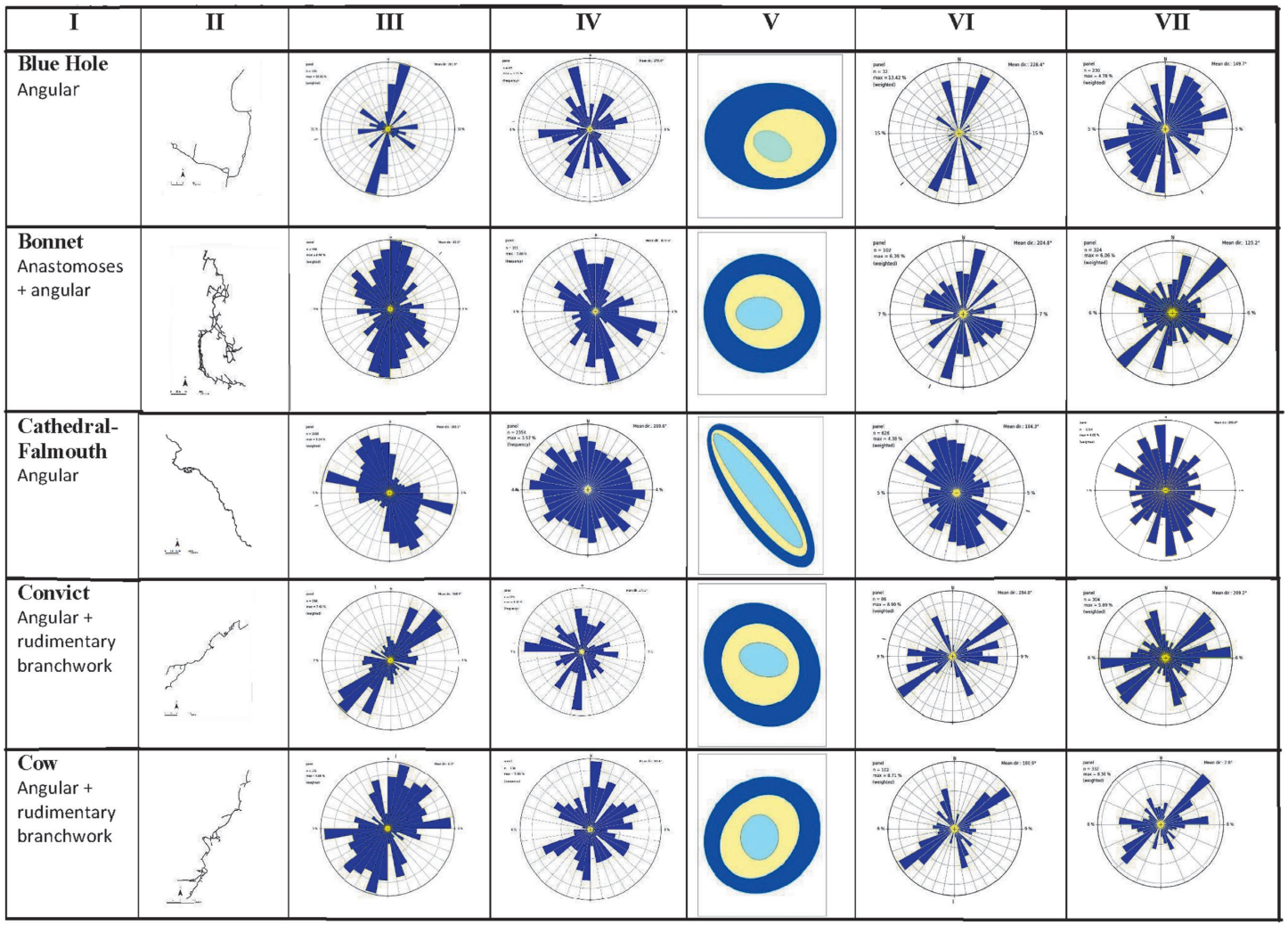

Figure 5a: Summary of Directional Analyses. I) Cave name and pattern, II) Cave passage centerline, III) Cave passages (% of total length), IV) Nearest neighbor azimuth for depression centroids within 2 km of the cave centerline (frequency) V) Standard Deviational Ellipses for depression centroids within 1, 2, and 3 km of cave centerlines, VI) Major axes (% of total length) for depressions with major axis/minor axis >= 1.5 within 2 km of the cave centerline, VII) Major axes (% of total length) for depressions with major axis/minor axis >= 1.5 within 3 km of the cave centerline.

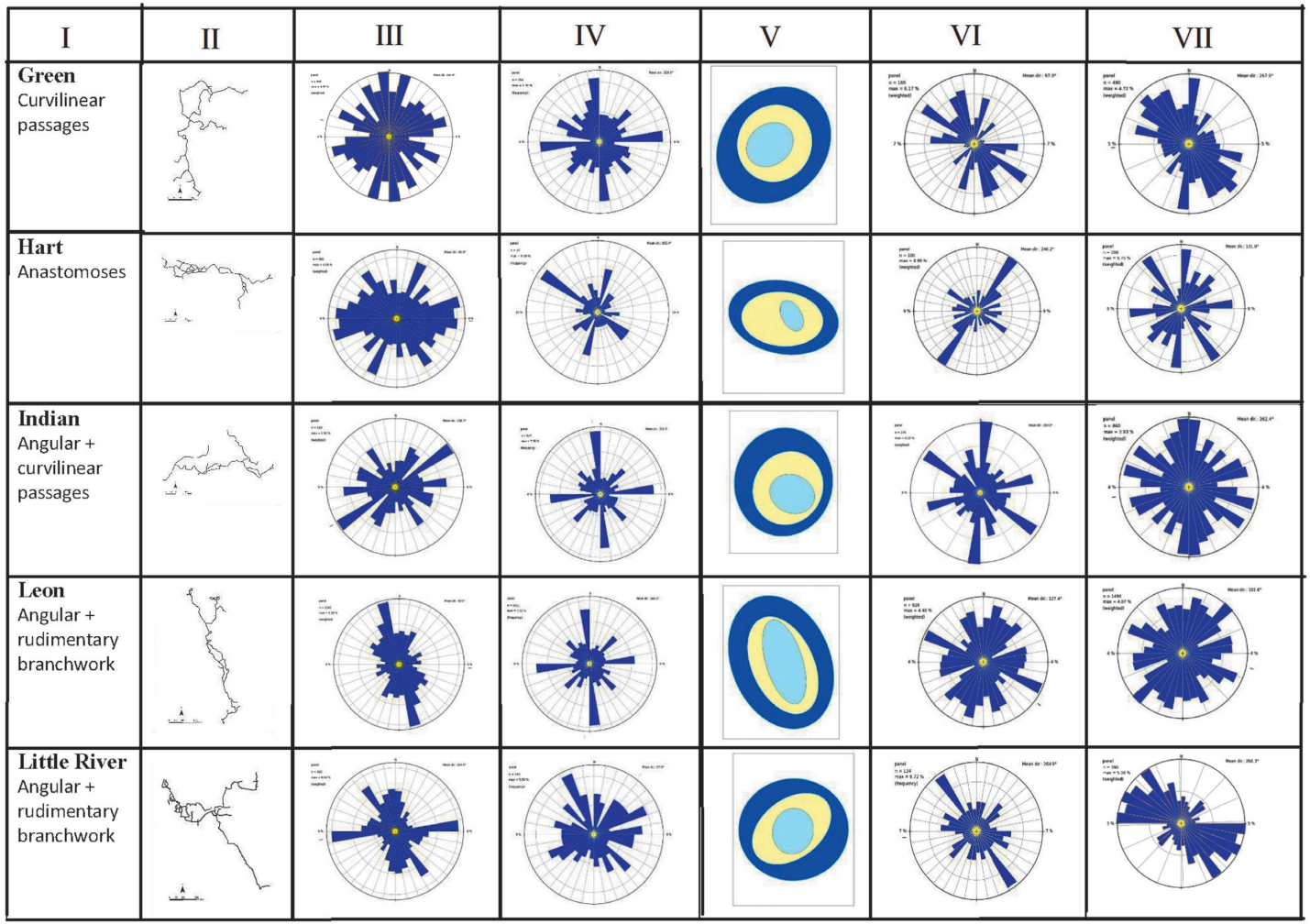

Figure 5.b: Summary of Directional Analyses. I) Cave name and pattern, II) Cave passage centerline, III) Cave passages (% of total length), IV) Nearest neighbor azimuth for depression centroids within 2 km of the cave centerline (frequency) V) Standard Deviational Ellipses for depression centroids within 1, 2, and 3 km of cave centerlines, VI) Major axes (% of total length) for depressions with major axis/minor axis >= 1.5 within 2 km of the cave centerline, VII) Major axes (% of total length) for depressions with major axis/minor axis >= 1.5 within 3 km of the cave centerline.

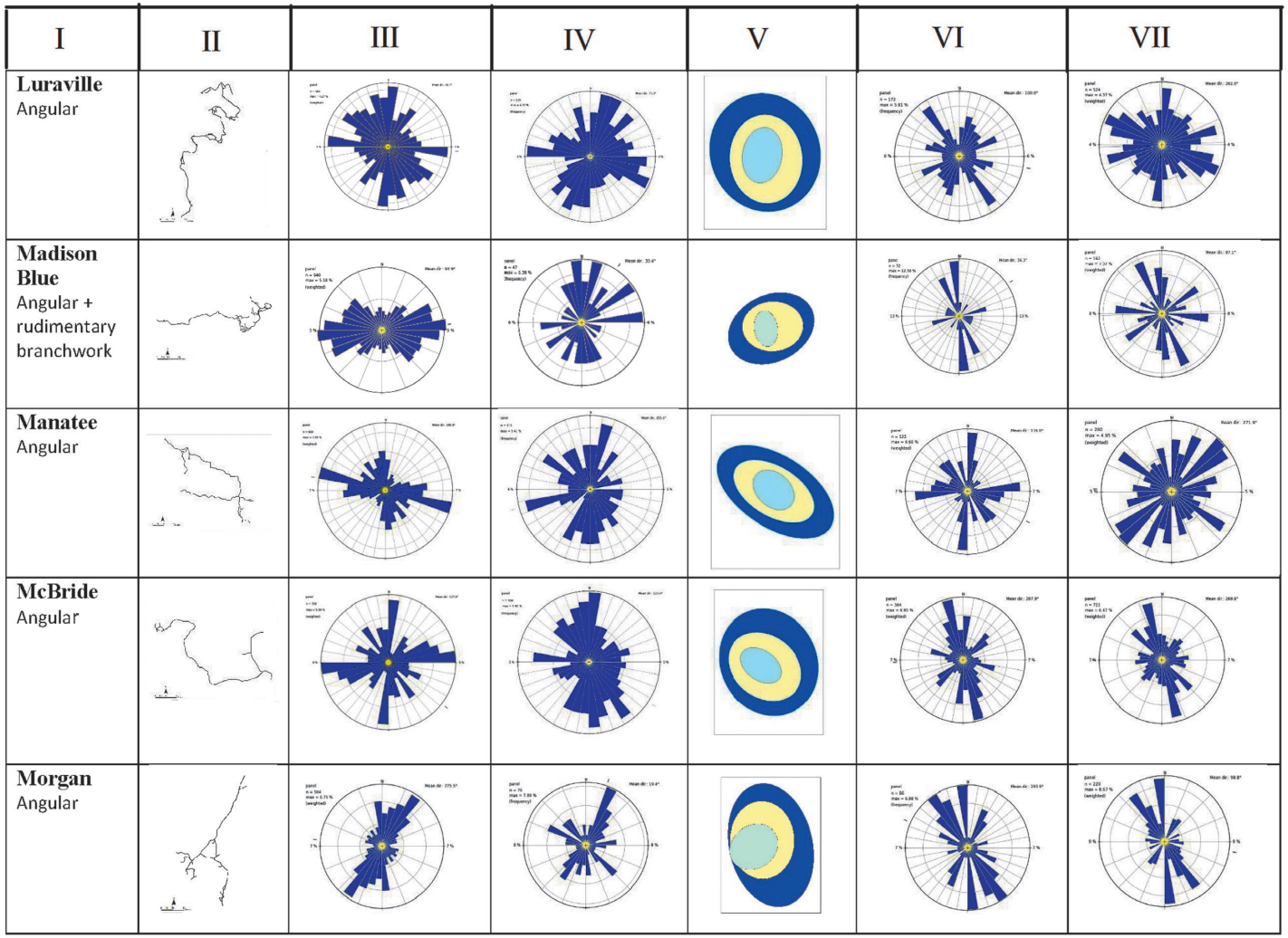

Figure 5c: Summary of Directional Analyses. I) Cave name and pattern, II) Cave passage centerline, III) Cave passages (% of total length), IV) Nearest neighbor azimuth for depression centroids within 2 km of the cave centerline (frequency) V) Standard Deviational Ellipses for depression centroids within 1, 2, and 3 km of cave centerlines, VI) Major axes (% of total length) for depressions with major axis/minor axis >= 1.5 within 2 km of the cave centerline, VII) Major axes (% of total length) for depressions with major axis/minor axis >= 1.5 within 3 km of the cave centerline.

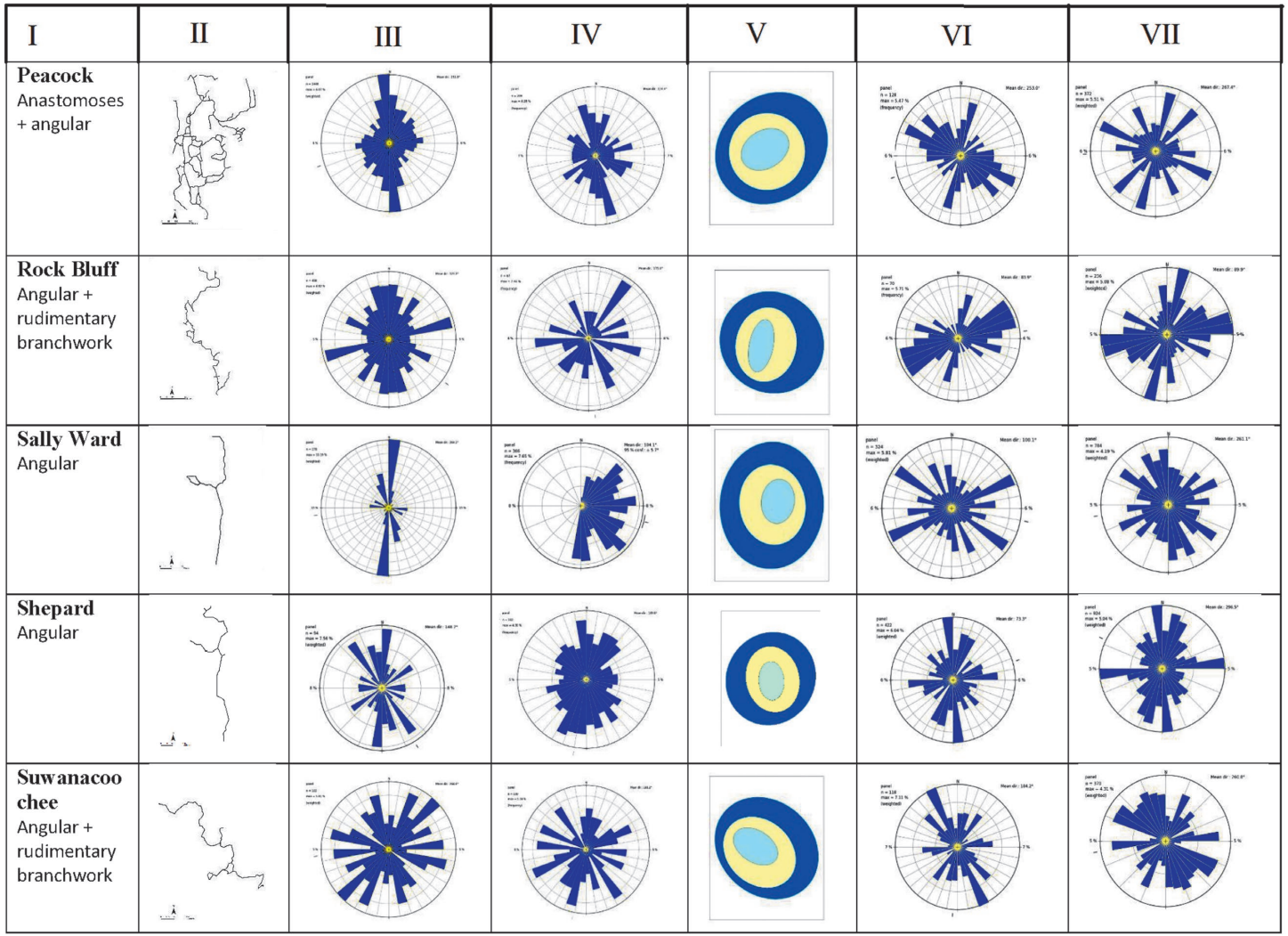

Figure 5d: Summary of Directional Analyses. I) Cave name and pattern, II) Cave passage centerline, III) Cave passages (% of total length), IV) Nearest neighbor azimuth for depression centroids within 2 km of the cave centerline (frequency) V) Standard Deviational Ellipses for depression centroids within 1, 2, and 3 km of cave centerlines, VI) Major axes (% of total length) for depressions with major axis/minor axis >= 1.5 within 2 km of the cave centerline, VII) Major axes (% of total length) for depressions with major axis/minor axis >= 1.5 within 3 km of the cave centerline.

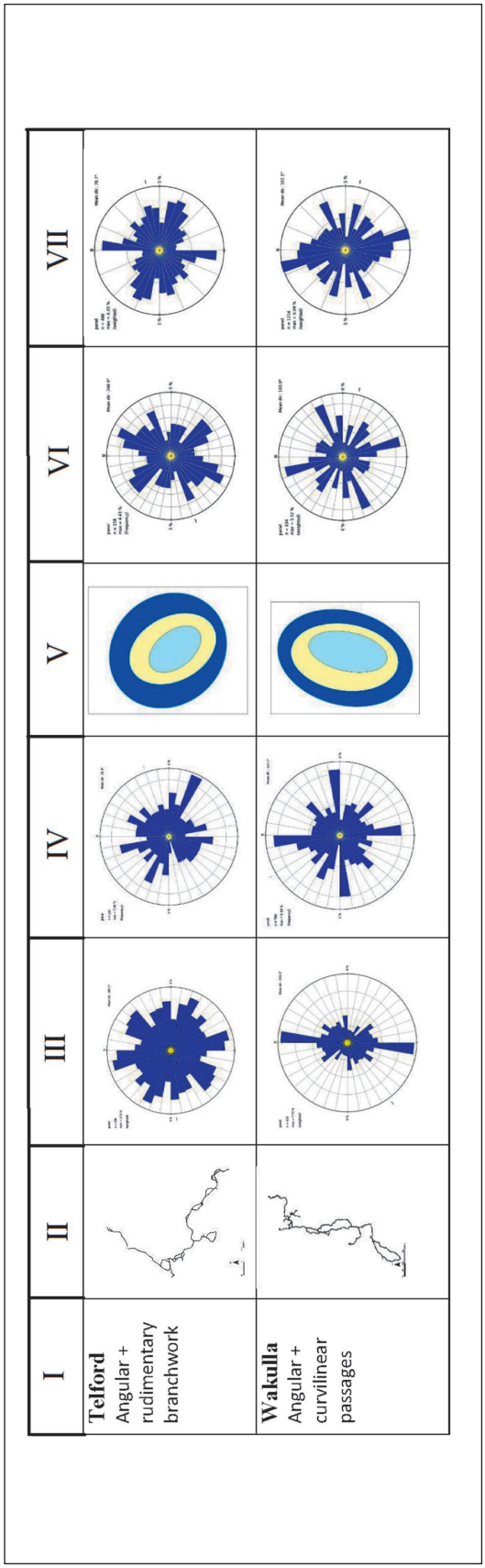

Figure 5e: Summary of Directional Analyses. I) Cave name and pattern, II) Cave passage centerline, III) Cave passages (% of total length), IV) Nearest neighbor azimuth for depression centroids within 2 km of the cave centerline (frequency) V) Standard Deviational Ellipses for depression centroids within 1, 2, and 3 km of cave centerlines, VI) Major axes (% of total length) for depressions with major axis/minor axis >= 1.5 within 2 km of the cave centerline, VII) Major axes (% of total length) for depressions with major axis/minor axis >= 1.5 within 3 km of the cave centerline.

Standard Deviational Ellipses of karstic depression centroids show wide variations in circularity. For example, major axis/minor axis ratios of SDEs for depressions within 3 km of each cave ranges from 1.04 for Bonnet cave to 2.99 for Cathedral-Falmouth cave system, indicating various degrees of spatial trends for the surficial karst features. Spatial distribution of depression centroids, as revealed by SDEs around cave centerlines, show moderate to good alignment with the centerlines of most of the caves except for Blue Hole, Bonnet, Convict, Green, Indian, and Peacock.

Along with a visual comparison of the rose diagrams for the depression major axes and the cave passages given in Figure 5, a statistical comparison was also tested using Kolmogorov-Smirnov (K-S) two-sample technique as applied by Barlow & Ogden (1982) (Table 2). The calculations, performed using the statistical package XLSTAT and verıfied by DGOF in R, allow us to infer if the two samples follow the same distribution. In this process, cave passage and depression major axis azimuths were compared as percentages of total length in 10-degree azimuth intervals. Except for the Sally's Ward and Madison Blue two-km data sets, all the cave alignments and surrounding major axes are interpreted to be following the same distribution as the calculated p values are greater than the significance level of 5% (alfa = 0.05). P values confirm high levels of correlation between the cave passage and depression major axis azimuths especially for Bonnet, Convict, Cow, Hart, Indian, Leon, Little River, Luraville, Manatee, Peacock, Suwanacoochee, and Wakulla.

Fracture control in cave development in Florida was mentioned in various studies. Florea (2006) describes cave passages along fractures with preferred orientations in WNW-ES (100-120) and NNE-SSW (20-40) in Brooksville Ridge, Florida. Similar fracture trends were reported by Vernon (1951) and Culton (1978). In this study, field measurements of joint systems along the Suwannee River show two distinct patterns (see the rose diagrams in Figure 6). While a NE/SW orientation is dominant along the upper Suwannee, fractures along the north-south stretch of the river trend in NW/SE orientation. These patterns generally conform with the cave development as well as the orientation of the Suwannee River's course.

Table 2: Results of the Kolmogorov-Smirnov analysis between the cave passage and sinkhole major axis orientations as percent of total length in 10-degree intervals. Data sets that do not follow the same distribution with a significance level of 0.05 are in bold.

Cave	Distance from the Cave	D	p-value (Two-tailed)
Blue Hole	2 km	0.39	0.13
	3 km	0.39	0.13
Bonnet	2 km	0.28	0.49
	3 km	0.17	0.96
Cathedral-Falmouth	2 km	0.28	0.49
	3 km	0.33	0.27
Convict	2 km	0.28	0.49
	3 km	0.17	0.96
Cow	2 km	0.28	0.49
	3 km	0.17	0.96
Green	2 km	0.39	0.13
	3 km	0.33	0.27
Hart	2 km	0.22	0.76
	3 km	0.22	0.76
Indian	2 km	0.33	0.27
	3 km	0.17	0.96
Leon	2 km	0.22	0.77
	3 km	0.33	0.27
Little River	2 km	0.22	0.76
	3 km	0.22	0.76
Luraville	2 km	0.28	0.49
	3 km	0.22	0.76
Madison Blue	**2 km**	**0.44**	**0.05**
	3 km	0.33	0.28
Manatee	2 km	0.17	0.96
	3 km	0.17	0.96
McBride	2 km	0.33	0.27
	3 km	0.31	0.39
Morgan	2 km	0.28	0.49
	3 km	0.33	0.27
Peacock	2 km	0.22	0.76
	3 km	0.33	0.27
Rock Bluff	2 km	0.28	0.49
	3 km	0.33	0.27
Sally's Ward	**2 km**	**0.5**	**0.02**
	3 km	**0.44**	**0.04**
Shepard	2 km	0.28	0.49
	3 km	0.33	0.27
Suwanacoochee	2 km	0.22	0.76
	3 km	0.17	0.96
Telford	2 km	0.44	0.06
	3 km	0.33	0.27
Wakulla	2 km	0.22	0.76
	3 km	0.16	0.6

Karst development in Florida is controlled not only by fracture systems and hydraulic gradients, but also by the type of porosity and the pattern of recharge to the carbonate bedrock. Allogenic recharge from non-karst areas accounts for extensive dissolution along the retreating escarpment, resulting in sinking streams and collapsed depressions above and around cave conduits with crude branchwork patterns. This pattern of karst development is further complicated by diffuse recharge through permeable soil cover on the bedrock, resulting in extensive epikarst-initiated cave development. In both types of recharge patterns, a connection between surface – subsurface karst development, and the effect of fracture systems are clear. In this study, this connection was established by an analysis of large data sets on caves and sinkholes on a GIS platform.

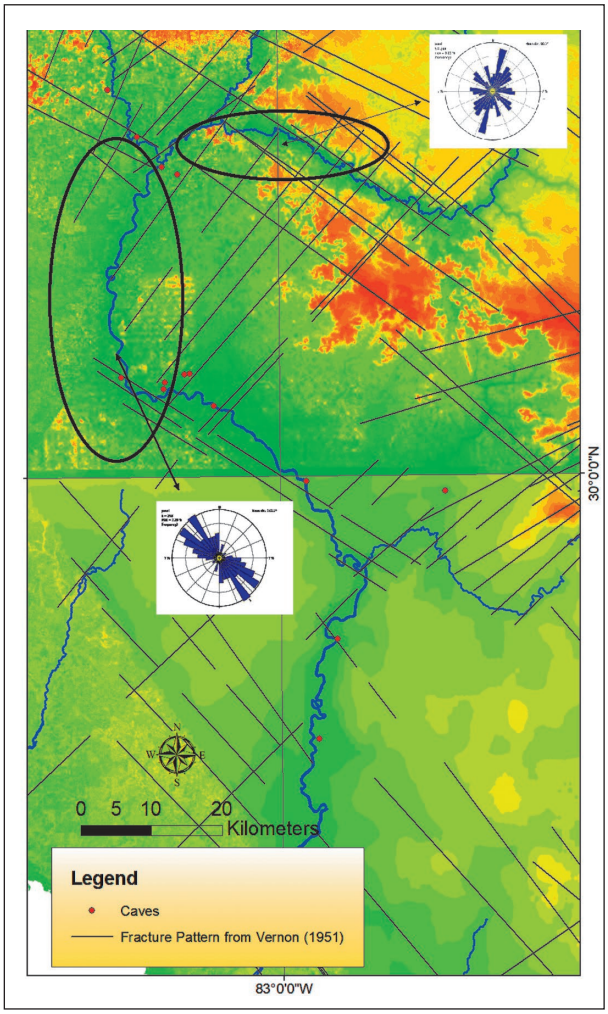

Figure 6: Fractures from Vernon (1951) and the rose diagrams for fracture azimuths along the Suwannee River. Ellipses show general areas of data collection.

6. SUMMARY

In order to explore the connection between surficial and subsurface karst development in Florida, spatial correlation of twenty-two cave passages and a large number of surrounding karstic depressions was carried out in a GIS-based spatial analysis (see Figure7 for an example of cave passage centerlines and the surrounding karstic depressions). Morphometric parameters evaluated in this study included cave passage orientations, depression major axis orientations, nearest neighbor depression directions, as well as spatial distribution patterns of depressions. Analysis of the data provides further support for the connection between the surficial and subsurface karst processes in the eogenetic karst of Florida. It also appears that the structural control plays an important role in karst development.

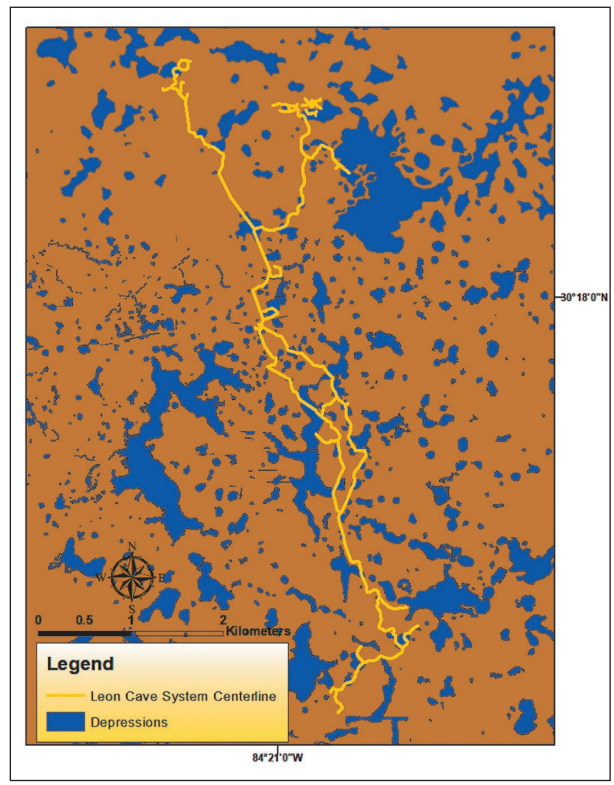

Figure 7: Leon Cave system and the surrounding karstic depressions.

REFERENCES

Angel, J., Nelson, D., Panno, S., 2004. Comparison of a new GIS-based technique and a manual method for determining sinkhole density: an example from Illinoi's sinkhole plain. Journal of Cave and Karst Studies, 66(1): 9-17.

Barlow, C., Ogden, A., 1982. A statistical comparison of joint, straight cave segment, and photo-lineament orientations. NSS Bulletin, 44: 107-110.

Culton, R., 1978. The subsurface geology of Hamilton County, Florida, with emphasis on the Oligocene age Suwannee Limestone. [MSc Thesis]. Florida State University, Tallahassee, 185 pp.

Denizman, C., Randazzo, A., 2000. Post-Miocene subtropical karst evolution, lower Suwannee River basin, Florida. GSA Bulletin, 112(12): 1804-1813.

Denizman, C., 2003. Morphometric and spatial distribution of karstic depressions, Lower Suwannee River Basin, Florida. Journal of Cave and Karst Studies, 65(1): 29-35.

Faivre, S., Pahernik, M., 2007. Structural influences on the spatial distribution of dolines, Island of Brac, Croatia. Zeitschrift für Geomorphologie, 51(4): 487-503.

Florea, L., 2006. Architecture of air-filled caves within the karst of the Brooksville Ridge, west-central Florida. Journal of Cave and Karst Studies, 68(2): 64-75.

Florea, L., Vacher, H., 2006. Cave levels, marine terraces, paleoshorelines, and the water table in Peninsular Florida. Archives of Climate Change in Karst, Karst Waters Institute Special Publication 10, 188-192 pp.

Ford, D., 1964. Origin of closed depressions in the central Mendip Hills, Somerset, England. In: Hamilton, F.E.I. (Eds.), Abstract of Papers, 20th International Geographical Congress, 6th July – 20th August 1964, London, pp. 105-106.

Gulley, J., Martin, J., Moore, P.J., Murphy, J., 2013. Formation of phreatic caves in and eogenetic karst aquifer by CO2 enrichment at lower water tables and

subsequent flooding by sea-level rise. Earth Surface Processes and Landforms, 38(1): 1210-1224. https://doi.org/10.1002/esp.3358

Kemmerly, P., 1982. Spatial analysis of a karst depression population: Clues to genesis. GSA Bulletin, 93(11): 1078–1086.

Kincaid, T., 1998. River water intrusion to the unconfined Floridan aquifer. Environmental and Engineering Geosciences, 4: 361-374.

Komac, M., Urbanc, J., 2012. Assessment of spatial properties of karst areas on a regional scale using GIS and statistics – the case of Slovenia. Journal of Cave and Karst Studies, 74(3): 261-261. https://doi.org/10.4311/2010ES0188R

La Valle, P., 1967. Some aspects of linear karst development in South Central Kentucky. Annals of the Association of American Geographers, 57(1): 49-71. https://doi.org/10.1111/j.1467-8306.1967.tb00590.x

Lyew-Ayee, P., Viles, H.A., Tucker, G.E., 2006. The use of GIS-based digital morphometric techniques in the study of cockpit karst.- Earth Surface Processes and Landforms, 32(2): 165-179. https://doi.org/10.1002/esp.1399

Mitchell, A., 2005. The ESRI guide to GIS analysis. Volume: 2 spatial measurements and Statistics. ESRI press, Redlands, California, 238 pp.

Moore, P., Martin, J., Screaton, E., Neuhoff, P., 2010. Conduit enlargement in eogenetic karst aquifer. Journal of Hydrology, 376(3-4): 143 – 155. https://doi.org/10.1016/j.jhydrol.2010.08.008

Öztürk, M., Şener, M., Şimşek, M., 2018. Structural controls on distribution of dolines on Mount Anamas (Taurus Mountains, Turkey). Geomorphology, 317: 107-116. https://doi.org/10.1016/j.geomorph.2018.05.023

Palmer, A., 1991. Origin and morphology of limestone caves. Geological Society of America Bulletin, 103: 1-21.

Palmer, A., 2009. Cave Geology. Cave Books, Dayton, 454 pp.

Palmer, M., Palmer, A., 1975. Landform development in the Mitchel Plain of southern Indiana: Origin of a partially karstified plain. Zeitschrift für Geomorphologie, 19: 1-39.

Randazzo, A, 1997. The sedimentary platform of Florida: Mesozoic to Cenozoic. In: Randazzo, A., Jones, D. (Eds.), Geology of Florida. University Press of Florida, Gainesville, Florida, pp. 39-56.

Shofner, G., Mills, H., Jason, E., 2001. A simple map index of karstification and its relationship to sinkhole and cave distribution in Tennessee. Journal of Cave and Karst Studies, 63(2): 67-75.

Scott, T.M., 1997. Miocene to Holocene history of Florida. In: Randazzo, A., Jones, D. (Eds.), Geology of Florida. University Press of Florida, Gainesville, Florida, pp. 57-68.

Upchurch, S., S. Thomas., M. Alfieri, B., Fratesi, Dobecki, T., 2019. The Karst Systems of Florida, Understanding Karst in a Geologically Young Terrain. Springer, New York, 450 pp.

Vacher, H., Mylroie, J., 2002. Eogenetic karst from the perspective of an equivalent porous medium. Carbonates and Evaporites, 17: 182-196.

Vernon, R., 1951. Geology of Citrus and Levy Counties, Florida. Florida Geological Survey Bulletin, 3, Florida Geological Survey, Tallahassee, Florida, 256 pp.

White, W., 1970. The Geomorphology of the Florida Peninsula. Florida Geological Survey Bulletin, 51, Florida Geological Survey, Tallahassee, Florida, 164 pp.